Measurements of projectile-like ^{8}Be and ^{9}B production in 200–400 MeV/nucleon ^{12}C on water

T. Toshito,[1,2] K. Kodama,[3] L. Sihver,[4] K. Yusa,[5] M. Ozaki,[6] K. Amako,[2] S. Kameoka,[2] K. Murakami,[2] T. Sasaki,[2] S. Aoki,[7] T. Ban,[8] T. Fukuda,[8] H. Kubota,[8] N. Naganawa,[8] T. Nakamura,[8] T. Nakano,[8] M. Natsume,[8] K. Niwa,[8] S. Takahashi,[8] J. Yoshida,[8] H. Yoshida,[9] M. Kanazawa,[10] N. Kanematsu,[10] M. Komori,[10] S. Sato,[10] M. Asai,[11] T. Koi,[11] C. Fukushima,[12] S. Ogawa,[12] M. Shibasaki,[12] and H. Shibuya[12]

[1]*CREST, Japan Science and Technology Agency, Kawaguchi 332-0012, Japan*
[2]*High Energy Accelerator Research Organization (KEK), Tsukuba 305-0801, Japan*
[3]*Aichi University of Education, Kariya 448-8542, Japan*
[4]*Chalmers University of Technology, SE-412 96 Gothenburg, Sweden and Roanoke College, Salem, Virginia 24153, USA*
[5]*Gunma University, Maebashi 371-8510, Japan*
[6]*Institute of Space and Astronautical Science, JAXA, Sagamihara 229-8510, Japan*
[7]*Kobe University, Kobe 657-8501, Japan*
[8]*Nagoya University, Nagoya 464-8602, Japan*
[9]*Naruto University of Education, Naruto 772-8502, Japan*
[10]*National Institute of Radiological Sciences (NIRS), Chiba 263-8555, Japan*
[11]*Stanford Linear Accelerator Center (SLAC), Stanford, California 94309, USA*
[12]*Toho University, Funabashi 274-8510, Japan*

(Received 15 July 2008; published 12 December 2008)

We have studied the production of the projectile-like fragments ^{8}Be and ^{9}B produced in interactions of 200 to 400 MeV/nucleon carbon ions with water, using emulsion detectors. In this Brief Report we present the first published production cross section of the projectile-like fragment ^{9}B in the energy region above 100 MeV/nucleon. The measured production cross sections of these nuclides were compared to calculations using a semiempirical model. We found that the measured cross sections deviate from the calculated values by a factor up to about six. This information is of importance for benchmarking and improving heavy ion nuclear reaction models.

DOI: 10.1103/PhysRevC.78.067602 PACS number(s): 25.70.Mn, 24.60.Ky

I. Introduction. Studies of the projectile fragmentation of artificially produced, highly energetic heavy ions have been carried out since the first acceleration of heavy ions at the Princeton Particle Accelerator and the Bevatron at the Lawrence Berkeley Laboratory in the early seventies. For energies above approximately 100 MeV/nucleon, the difference in rapidity between the projectile and the target fragments produced from peripheral collisions is clearly seen. The cross section to produce a particular nuclide as a projectile fragment is one of the key parameters needed to understand the reaction mechanism. Measurements have therefore been performed for a variety of combinations of beams and targets [1]. The results have been used to validate the fragmentation cross section model developed by Sihver *et al*. [2] at beam energies above ∼100 MeV/nucleon. This model is used, for example, in the one-dimensional particle and transport code HIBRAC [3].

Previously, only a few experiments studying the projectile ^{8}Be fragment at energies above 100 MeV/nucleon have been reported [4–6]. Because the lifetime of the ground state of ^{8}Be(^{8}Be$_{g.s.}$) is too short (7×10^{-17} s) to track, the mass of these isotopes cannot be determined with magnetic spectrometers or Cherenkov counters. In the experiments reported in these publications, emulsions were used as both target and tracking device, and the ^{8}Be$_{g.s.}$ signal was taken from the angular correlation between two projectile-like α fragments. No experimental results for projectile ^{9}B fragments with energies above 100 MeV/nucleon have been reported. The ground state of ^{9}B(^{9}B$_{g.s.}$) has a short lifetime (8.5×10^{-19} s) and decays into a ^{8}Be$_{g.s.}$ and a proton.

We have studied carbon ion fragmentation with emulsion technology at NIRS-HIMAC in Japan and recently reported the charge-changing cross sections for 200–400 MeV/nucleon ^{12}C in water [7]. Using the same data sets, we have now analyzed the angular correlation between the light fragments to study ^{8}Be$_{g.s.}$ and ^{9}B$_{g.s.}$ production.

In this article, we report measurements of ^{8}Be$_{g.s.}$ and ^{9}B$_{g.s.}$, produced as projectile fragments in the interactions of ^{12}C on water in the energy region 200–400 MeV/nucleon. The production cross sections have been compared with model calculations [2].

II. Experiment and analysis. The Emulsion Cloud Chamber (ECC) was designed to store the products of all fragmentation reactions. A schematic drawing of the chamber is shown in Fig. 1. It was constructed from 65 emulsion module layers with 2-mm-thick gaps separating adjacent layers. The gaps were filled with deionized water at the time of exposure. Each emulsion module layer consisted of a stack of four emulsion sheets, reinforced with a 1.05-mm-thick polycarbonate plate and then vacuum-packed in an aluminum-coated film for light- and waterproofing.

A pair of emulsion sheets was placed on each side of the polycarbonate plate as shown in Fig. 1(b).[1] The emulsion sheet itself measured 102 mm by 127 mm and was made of OPERA film [8], consisting of a 205-μm-thick TAC (cellulose

[1]The emulsion sheets in each module are labeled "A" through "D" as shown in Fig. 1(b).

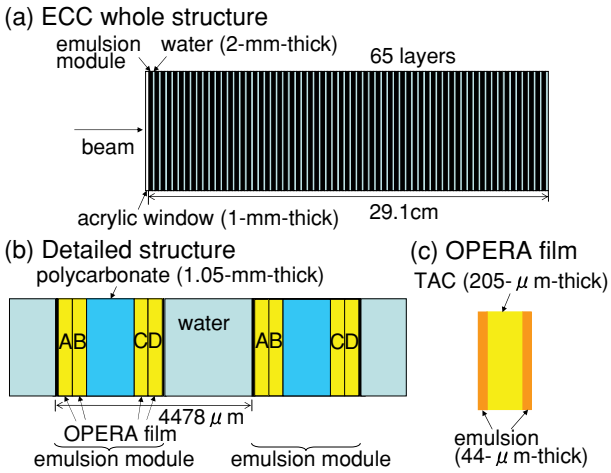

FIG. 1. (Color online) (a) Schematic view of the Emulsion Cloud Chamber (ECC). It has 65 layers of emulsion modules interspersed with water targets. (b) Detailed structure of the ECC. An emulsion module consists of four emulsion sheets and a polycarbonate plate. (c) Cross section of an OPERA film. An OPERA film consists of a TAC base coated on both sides with an emulsion layer.

triacetate) base, coated on both sides with 44-μm-thick emulsion layers. This detail is shown in Fig. 1(c).

Details of the detector, data reduction, and analysis can be found in Ref. [7].

We exposed the chamber to 400 MeV/nucleon ^{12}C in the SB2 beam line [9] of the HIMAC heavy ion synchrotron in December 2004. The total count of beam tracks was 24 237. After the exposure, sheets A and C were developed normally and sheets B and D were processed applying the so-called refreshing method [10] before development. Refreshing is a technology used to desensitize emulsions by means of forced fading. It extends the dynamic range of response to highly charged particles.

The emulsion scanning was performed by fully automated Ultra Track Selector (UTS) [11] microscopes. The track-finding efficiency of the UTS was 98%. The UTS records the grain density of each track segment as a pulse height, thus storing the local deposited energy. The positional and angular resolutions of a track were found to be 1 μm and 1 mrad, respectively. We obtained 8213 fragmentation reactions at beam energies ranging from 200 to 400 MeV/nucleon. Reconstructed vertex positions were used to select the $^{12}C + H_2O$ interactions.

III. Results. A. ^{8}Be$_{g.s.}$ *production.* When ^{8}Be$_{g.s.}$ is produced as a projectile-like fragment, its velocity is equal to that of the primary carbon ion to within a few percent error. The fragment promptly decays into two forward-going α particles with a maximum opening angle of 0.013 rad. This angle is due kinematically to the mass difference of 92 keV between ^{8}Be$_{g.s.}$ and two α particles.

In this experiment the charge of each individual track was identified by using the combination of pulse heights measured in the films processed by different refreshing treatments [7,10]. Helium particles with tangents of the polar angle less than 0.1 were identified with more than 95% purity. We selected the fragmentation reactions that had more than one secondary

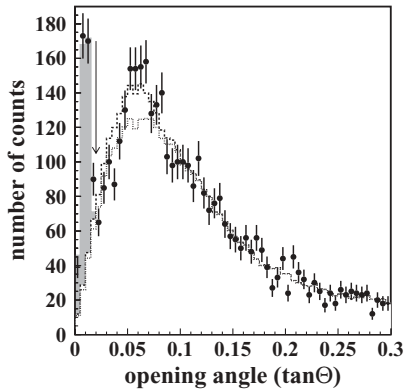

FIG. 2. Opening angle between two helium particles ($\Theta_{\alpha\alpha}$). (Black dots) Data and statistical errors. The cut point to select ^{8}Be$_{g.s.}$ events is indicated by the arrow. (Dotted histogram) Background events with best fit parameters. (Dashed histogram) The sum of ^{8}Be$^*_{3.04}$ and background events with best fit parameters. (Gray histogram) ^{8}Be$_{g.s.}$ events with best fit parameters.

helium particle and obtained 3188 events at beam energies ranging from 200 to 400 MeV/nucleon.

Figure 2 shows the measured distribution of opening angles between two helium particles ($\Theta_{\alpha\alpha}$). Here, we consider any combination of two helium particles for each event. A prominent peak at $\Theta_{\alpha\alpha} \sim 0.01$ corresponds to the value expected for the fragments originating from the decays of the ^{8}Be$_{g.s.}$. It contains 472 events in the region of $\Theta_{\alpha\alpha} < 0.020$. ^{8}Be$_{g.s.}$ events are well contained considering the error of the track angle measurement. There is also a broad background with a peak at $\Theta_{\alpha\alpha} \sim 0.06$.

We suppose that there is no angular correlation between two background helium particles and that the $\Theta_{\alpha\alpha}$ distribution of the broad background is the same as the $\Theta_{\alpha\alpha}$ distribution obtained by selecting helium particles from different events. We also consider the contribution of the production of the first excited state of ^{8}Be (^{8}Be$^*_{3.04}$). ^{8}Be$^*_{3.04}$ promptly decays into two α particles and their opening angle distribution has a peak at $\Theta_{\alpha\alpha} \sim 0.06$.

To estimate the yield of ^{8}Be$_{g.s.}$ production the opening angle distribution was fitted with a combination of the expected signal distributions from ^{8}Be$_{g.s.}$, ^{8}Be$^*_{3.04}$, and background. The fitted opening angle distribution and χ^2, which is minimized, are

$$\chi^2 = \sum_{\Theta_{\alpha\alpha_i}}^{60} \frac{\left(N_i^{\rm obs} - \alpha N_i^A - \beta N_i^B - \gamma N_i^C\right)^2}{\sigma_i^2}, \qquad (1)$$

where $N_i^{\rm obs}$ is the number of observed events, N_i^A is the number of ^{8}Be$_{g.s.}$ events, N_i^B is the number of ^{8}Be$^*_{3.04}$ events, N_i^C is the number of background events, and σ_i is the statistical error for the ith bin. The opening angle distribution was divided into 60 bins from 0 to 0.3, and the sample normalizations, α, β, and γ, were allowed to vary freely. The distributions of $\Theta_{\alpha\alpha}$ for ^{8}Be$_{g.s.}$ and ^{8}Be$^*_{3.04}$ were produced by a Monte Carlo simulation considering the energy distribution of the beam energy and the measurement error of the secondary track angle. The results of the fit are shown in Fig. 2. The number of ^{8}Be$_{g.s.}$ events was

TABLE I. ^{8}Be production cross sections for ^{12}C beams in a water target.

Energy (MeV/nucleon)	$\sigma_{^8\mathrm{Be}} + \sigma_{^9\mathrm{B}}$ (mb) Our results	$\sigma_{^8\mathrm{Be}}$ (mb)	
		Our results	Ref. [2]
364 ± 25	33^{+7}_{-6}	22^{+7}_{-6}	140
312 ± 27	42^{+8}_{-7}	31^{+8}_{-7}	159
255 ± 30	39^{+9}_{-8}	28^{+9}_{-8}	177

found to be 301 ± 19. There is some excess of data above the fitted line around $\Theta_{\alpha\alpha} \sim 0.06$. It is likely due to an imperfect understanding of the background distribution.[2] However, we assume that these effects on the estimation of signal yield can be neglected.

We selected the $^{12}\mathrm{C} + \mathrm{H_2O}$ reaction and calculated the production cross sections of projectile $^{8}\mathrm{Be}_{\mathrm{g.s.}}$ fragments and their statistical errors. We note that the $^{8}\mathrm{Be}_{\mathrm{g.s.}}$ events include both the events in which $^{8}\mathrm{Be}_{\mathrm{g.s.}}$ are directly produced as projectile-like fragments and the events in which $^{8}\mathrm{Be}_{\mathrm{g.s.}}$ are produced as decay daughters of $^{9}\mathrm{B}_{\mathrm{g.s.}}$ produced as projectile-like fragments. The latter, i.e., production of projectile $^{9}\mathrm{B}_{\mathrm{g.s.}}$ fragments, is discussed in the next subsection. We first calculated the sum of $^{8}\mathrm{Be}_{\mathrm{g.s.}}$ and $^{9}\mathrm{B}_{\mathrm{g.s.}}$ production cross sections from the number of $^{8}\mathrm{Be}_{\mathrm{g.s.}}$ events. Then the $^{8}\mathrm{Be}_{\mathrm{g.s.}}$ production cross section was calculated by subtracting the $^{9}\mathrm{B}_{\mathrm{g.s.}}$ production cross section, which is described in the next subsection. The results are summarized in Table I.

The systematic error consists of the following components: the uncertainty in vertex positions, which affects the position cut when selecting a target material, resulted in an uncertainty of 3%; the probability of charge misidentification of primary or secondary particles was estimated to add an uncertainty of 3%; the inefficiency for detecting two secondary α particles contributed a systematic uncertainty of 4%; the contamination of ^{10}C and ^{11}C in the ^{12}C beam was expected to contribute an uncertainty of 3%. The quadrature sum of all these uncertainties yielded a total estimated systematic error of 7%. The details of how these uncertainties were estimated are described in Ref. [7].

We note that although we cannot identify the mass of the fragments, $^{8}\mathrm{Be}_{\mathrm{g.s.}} \rightarrow \alpha + \alpha$ is the only reaction that can produce a peak in the region of $\Theta_{\alpha\alpha} < 0.020$. The possibilities of a peak in this region resulting from two ^{3}He or a ^{3}He and an α particle were ruled out by earlier studies done at energies below 100 MeV/nucleon [12].

B. $^{9}\mathrm{B}_{\mathrm{g.s.}}$ *production.* We performed further analysis of the events selected as $^{8}\mathrm{Be}_{\mathrm{g.s.}}$ production to detect $^{9}\mathrm{B}_{\mathrm{g.s.}}$. $^{9}\mathrm{B}_{\mathrm{g.s.}}$ produced as a projectile fragment has a velocity equal to within a few percent error to that of the the primary carbon ion and promptly decays into a proton and $^{8}\mathrm{Be}_{\mathrm{g.s.}}$. Furthermore, $^{8}\mathrm{Be}_{\mathrm{g.s.}}$ promptly decays into two α particles: $^{9}\mathrm{B}_{\mathrm{g.s.}} \rightarrow \mathrm{p} + {}^{8}\mathrm{Be}_{\mathrm{g.s.}} \rightarrow \mathrm{p} + (\alpha + \alpha)$. The proton and two α particles are all forward-going, with the maximum opening angle between the proton and $^{8}\mathrm{Be}_{\mathrm{g.s.}}$ being 0.03 rad in the energy region above 200 MeV/nucleon. This is due kinematically to the mass difference between $^{9}\mathrm{B}_{\mathrm{g.s.}}$ and the proton and $^{8}\mathrm{Be}_{\mathrm{g.s.}}$, which is 185 keV. We selected the fragmentation reactions in which at least one proton and more than one secondary α particle were produced and obtained 2663 events at beam energies ranging from 200 to 400 MeV/nucleon.

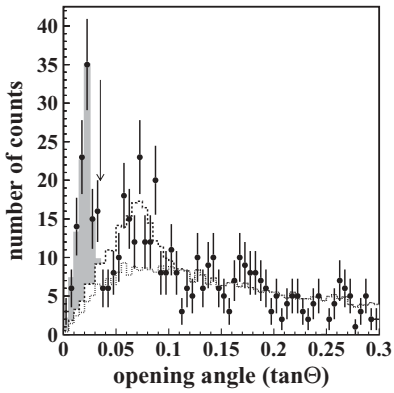

FIG. 3. Distribution of $\Theta_{p\alpha\alpha}$ after removing events containing $^{8}\mathrm{Be}_{\mathrm{g.s.}}$. (Black dots) Data and statistical errors. The cut point to select $^{9}\mathrm{B}_{\mathrm{g.s.}}$ events is indicated by the arrow. (Dotted histogram) Background events with best fit parameters. (Dashed histogram) The sum of $^{9}\mathrm{B}^{*}_{2.36}$ and background events with best fit parameters. (Gray histogram) $^{9}\mathrm{B}_{\mathrm{g.s.}}$ events with best fit parameters.

Here, we consider the opening angle of $\Theta_{p\alpha\alpha}$ determined by the direction of one proton ($\vec{t}_1$) and two α particles ($\vec{t}_2$, $\vec{t}_3$). $\vec{t}_{23}$ is defined as the average of the directions of two α particles: $\vec{t}_{23} \equiv (\vec{t}_2 + \vec{t}_3)/2$. The direction of $\vec{t}_{23}$ corresponds to the direction of $^{8}\mathrm{Be}_{\mathrm{g.s.}}$. $\Theta_{p\alpha\alpha}$ is defined as the opening angle between $\vec{t}_1$ and $\vec{t}_{23}$. Figure 3 shows the distribution of $\Theta_{p\alpha\alpha}$ after cutting events that have $^{8}\mathrm{Be}_{\mathrm{g.s.}}$, i.e., $\Theta_{\alpha\alpha} < 0.020$. All combinations of $\vec{t}_1, \vec{t}_2$, and $\vec{t}_3$ all allowed for each event. The prominent peak at $\Theta_{p\alpha\alpha} \sim 0.02$ corresponds to the two-stage decay of $^{9}\mathrm{B}_{\mathrm{g.s.}}$. It contains 112 events in the region of $\Theta_{p\alpha\alpha} < 0.035$. $^{9}\mathrm{B}_{\mathrm{g.s.}}$ events are well contained in this region considering the error in the track angle measurement. There is also a broad background.

We suppose that the broad background distribution of $\Theta_{p\alpha\alpha}$ is the same as the $\Theta_{p\alpha\alpha}$ distribution obtained in events that do not contain $^{8}\mathrm{Be}_{\mathrm{g.s.}}$ production, i.e., $\Theta_{\alpha\alpha} > 0.020$. We also considered the contribution of the production and two-stage decay of $^{9}\mathrm{B}^{*}_{2.36}$: $^{9}\mathrm{B}^{*}_{2.36} \rightarrow \alpha + {}^{5}\mathrm{Li} \rightarrow \alpha + (\mathrm{p} + \alpha)$. The opening angle distribution is expected to have a peak at $\Theta_{p\alpha\alpha} \sim 0.07$.

To estimate the yield of $^{9}\mathrm{B}_{\mathrm{g.s.}}$ production, the opening angle distribution is fitted with a combination of the expected signal distributions from $^{9}\mathrm{B}_{\mathrm{g.s.}}$, $^{9}\mathrm{B}^{*}_{2.36}$, and background. The fitted opening angle distribution and χ^2, which is minimized, are

$$\chi^2 = \sum_{\Theta_{p\alpha\alpha_i}}^{60} \frac{\left(N_i^{\mathrm{obs}} - \alpha N_i^A - \beta N_i^B - \gamma N_i^C\right)^2}{\sigma_i^2}, \qquad (2)$$

[2]In the next subsection we discuss the production and two-stage decay of $^{9}\mathrm{B}^{*}_{2.36}$. This mode is expected to have a peak at around 0.025 in the distribution of $\Theta_{\alpha\alpha}$. Therefore, the excess of data around $\Theta_{\alpha\alpha} \sim 0.06$ cannot be explained by this mode.

TABLE II. ^{9}B production cross sections for ^{12}C beams in a water target.

Energy (MeV/nucleon)	$\sigma_{^9\mathrm{B}}$ (mb)	
	Our results	Ref. [2]
307 ± 82	$11.3^{+2.5}_{-2.0}$	47

where N_i^{obs} is the number of observed events, N_i^A is the number of $^{9}\mathrm{B}_{\mathrm{g.s.}}$ events, N_i^B is the number of $^{9}\mathrm{B}^{*}_{2.36}$ events, N_i^C is the number of background events, and σ_i is the statistical error for the ith bin. The opening angle distribution was divided into 60 bins from 0 to 0.3, and the sample normalizations, α, β, and γ, were allowed to vary freely. The distributions of $\Theta_{p\alpha\alpha}$ for $^{9}\mathrm{B}_{\mathrm{g.s.}}$ and $^{9}\mathrm{B}^{*}_{2.36}$ were produced by a Monte Carlo simulation. The results of the fit are shown in Fig. 3. The number of $^{9}\mathrm{B}_{\mathrm{g.s.}}$ events was found to be 75 ± 10.

We selected the $^{12}\mathrm{C} + \mathrm{H_2O}$ reaction and calculated the production cross sections of the projectile $^{9}\mathrm{B}_{\mathrm{g.s.}}$ fragments and their statistical errors. The results are presented in Table II. The total systematic error was estimated to be 8% in a method similar to that used for the production cross section of $^{8}\mathrm{Be}_{\mathrm{g.s.}}$. The difference from the $^{8}\mathrm{Be}_{\mathrm{g.s.}}$ case comes from an increased uncertainty of 6% due to the required detection of an additional secondary proton.

We note that although we cannot identify the mass of the fragments, the two-stage decay of $^{9}\mathrm{B}_{\mathrm{g.s.}}$ is the only way to explain the peak in the region $\Theta_{p\alpha\alpha} < 0.035$. The possibility of a peak in this region due to ^{3}He, d, or t is ruled out by past low energy experiments [12].

IV. Discussion and conclusion. We have measured the production cross sections for projectile fragments $^{8}\mathrm{Be}_{\mathrm{g.s.}}$ and $^{9}\mathrm{B}_{\mathrm{g.s.}}$ from ^{12}C beams incident on water in the energy region 200–400 MeV/nucleon. Our results include the first observation of the $^{9}\mathrm{B}_{\mathrm{g.s.}}$ projectile above 100 MeV/nucleon. We compared the measured cross sections with calculations using a model developed by Sihver *et al.* [2]. The Sihver model is a semiempirical model that takes advantage of the experimentally verified weak factorization property [13] and can well reproduce the experimental data that were available when this model was developed. The measured and calculated cross sections are presented in Tables I and II. On average, Sihver's cross section model overestimates the cross sections by factors of approximately six (four) for the production of $^{8}\mathrm{Be}_{\mathrm{g.s.}}$ ($^{9}\mathrm{B}_{\mathrm{g.s.}}$). It is natural that there is such a large discrepancy because our results are the first to measure the production cross sections of these two nuclides. Additional measurements for various beams and targets combinations will improve the understanding of the reaction mechanism and of the cross section models.

The authors thank Dr. Nakahiro Yasuda of NIRS for useful suggestions and Dr. Dennis Wright of SLAC for careful reading of the manuscript. This research was performed as a Research Project with Heavy Ions at NIRS-HIMAC. This work was also supported in part by CREST of the Japan Science and Technology Agency (JST).

[1] See, for example, D. L. Olson, B. L. Berman, D. E. Greiner, H. H. Heckman, P. J. Lindstrom, G. D. Westfall, and H. J. Crawford, Phys. Rev. C **24**, 1529 (1981); J. M. Kidd, P. J. Lindstrom, H. J. Crawford, and G. Woods, *ibid.* **37**, 2613 (1988); W. R. Webber, J. C. Kish, and D. A. Schrier, *ibid.* **41**, 547 (1990).

[2] L. Sihver, C. H. Tsao, R. Silberberg, T. Kanai, and A. F. Barghouty, Phys. Rev. C **47**, 1225 (1993).

[3] L. Sihver, D. Schardt, and T. Kanai, Jpn. J. Med. Phys. **18**, 1 (1998); L. Sihver and D. Mancusi "HIBRAC: a 1-D deterministic heavy-ion transport code optimised for radiotherapy" (accepted for publication to Radiat. Meas.).

[4] A. El-Naghy, Z. Phys. A **302**, 261 (1981).

[5] V. V. Belaga, A. I. Bondarenko, Sh. A. Rustamova, and G. M. Chernov, Phys. At. Nucl. **59**, 1198 (1996).

[6] N. P. Andreeva *et al.*, Eur. Phys. J. A **27**, s01, 295 (2006).

[7] T. Toshito *et al.*, Phys. Rev. C **75**, 054606 (2007).

[8] K. Kuwabara and S. Nishiyama, J. Soc. Photogr. Sci. Technol. Jpn. **67**, 521 (2004); T. Nakamura *et al.*, Nucl. Instrum. Methods A **556**, 80 (2006).

[9] M. Kanazawa *et al.*, Nucl. Phys. **A746**, 393c (2004); Y. Iseki *et al.*, Phys. Med. Biol. **49**, 3179 (2004).

[10] T. Toshito *et al.*, Nucl. Instrum. Methods A **556**, 482 (2006).

[11] S. Aoki *et al.*, Nucl. Instrum. Methods B **51**, 466 (1990); T. Nakano, in Proceedings of International Workshop on Nuclear Emulsion Techniques, Nagoya, Japan, 1998; in Proceedings of International Europhysics Conference on High Energy Physics, Budapest, Hungary, 2001.

[12] See, for example, J. Pochodzalla *et al.*, Phys. Rev. C **35**, 1695 (1987); P. A. DeYoung *et al.*, *ibid.* **39**, 128 (1989); M. S. Gordon *et al.*, *ibid.* **46**, R1 (1992).

[13] D. L. Olson, B. L. Berman, D. E. Greiner, H. H. Heckman, P. J. Lindstrom, and H. J. Crawford, Phys. Rev. C **28**, 1602 (1983).